Mammalian skeletal muscle fibers distinguished by contents of phosphocreatine, ATP, and P_i

(fiber types/inorganic phosphate/adenosine triphosphate)

MARTIN J. KUSHMERICK*†‡, TIMOTHY S. MOERLAND§, AND ROBERT W. WISEMAN*

Departments of *Radiology and of †Physiology and Biophysics, University of Washington, Seattle, WA 98105; and §Department of Biological Science, Florida State University, Tallahassee, FL 32306

ABSTRACT We tested the proposition that muscle cell types have different contents of phosphocreatine (PCr), ATP, and P_i by ^{31}P NMR spectroscopy and HPLC analyses of adult rat and mouse muscles containing various volume fractions of different fiber types. There was a 2-fold difference in the PCr content between muscles with a high volume fraction of fiber types 1 and 2x versus those with fast-twitch (types 2a and 2b) fiber types. P_i content was low, and PCr and ATP contents were high in muscles with large contents of type 2b and 2a fibers; the reverse was true in muscles with a large volume fraction of type 1 and 2x fibers. There is a large range in the P_i/PCr ratios in normal resting muscles, from <0.05 in type 2 to 0.51 in type 1 fibers, depending upon the distribution of their component fiber types. In all muscles, the peak area resulting from the β phosphate of ATP constituted ≈13% of the sum of all peak areas observable in the ^{31}P spectrum. Fiber types 2a and 2b were not distinguishable, and the content of type 2x fibers was similar to type 1 fibers. From the profile of these metabolites, we could distinguish only two classes of fibers. For type 2a and 2b fibers, the intracellular concentrations were 8 mM ATP, 39 mM total creatine, 32 mM PCr, 0.8 mM P_i, and 8 μM ADP. For type 1 and 2x fibers, these quantities were 5 mM ATP, 23 mM total creatine, 16 mM PCr, 6 mM P_i, and 11 μM ADP. Thus our results establish an additional criterion upon which to distinguish skeletal muscle cells, one based on the resting content of bioenergetically important metabolites. These results also provide the basis for estimating skeletal muscle fiber-type composition from noninvasive NMR spectroscopic data.

Individual cells (also called fibers) in muscles can be classified by a number of anatomical, physiological, and biochemical methods (1) into various categories: (*i*) fatigue-sensitivity and recruitment order of individual motor units (2–4); (*ii*) oxidative, glycolytic, and mixed oxidative-glycolytic types based on histochemical staining of characteristic enzymes in the cells (5); and (*iii*) fast- and slow-twitch types, or types 1 and 2 (and further subtypes), based on myosin ATPase staining intensity (6, 7), mechanical properties (8–10), and myosin heavy- and light-chain isoform composition by immunochemistry and gel electrophoresis (11–16). Although the number of possible cell types is very large (1, 17), individual muscles with predominantly one characteristic can be obtained, and their energy metabolic and other functions can be studied (18) as recognized by Ranvier (19).

The ratio of inorganic phosphate (P_i) to phosphocreatine (PCr) or the ratio $P_i/(PCr + P_i)$ is often used to infer the bioenergetic status of a muscle in human exercise. The following evidence suggests that muscle fibers differ with respect to their contents of PCr, creatine, ATP, and P_i. Measurements of metabolite composition by ^{31}P NMR dem-

onstrated higher PCr and lower P_i contents in the feline biceps muscle than in the soleus muscle (SOL), and this compositional difference corresponded to the predominance of slow-twitch fibers in the SOL and their absence in the biceps (20). Chemical analyses of single-fiber segments dissected from resting and stimulated rat plantaris muscle and SOL (21) showed correlations among fiber types with metabolite content at rest as well as with the extent of PCr and ATP splitting during stimulation. The mechanistic basis for the differences in metabolite concentrations was attributed to the greater average rate of neural activation of type 1 fibers in the animal compared with type 2 fibers. Thus the reduced content of PCr and ATP was explained by increased muscle activity, not by a phenotypic characteristic. An alternative possibility—namely, that there are characteristic differences among fiber types in their content of PCr, ATP, and other metabolites at rest—has not been fully considered. We therefore designed experiments to test the hypothesis that there are significant differences in bioenergetically important metabolites in the major classes of fiber types.

METHODS

Muscle Preparation. We studied the extensor digitorum longus muscle (EDL), the SOL, the tensor fascia lata muscle (TFL), and the diaphragm muscle (DPH) dissected from 150- to 250-g Sprague–Dawley rats anesthetized with pentobarbital (60 mg/kg i.p.). We also studied EDL and SOL from 25- to 40-g Swiss–Webster mice. The component fiber types in the adult muscles that we chose for study were identified and classified into types 2b, 2a, 2x, or 1; the volume fraction of each muscle studied is listed in Table 1. Because the wet weight of some of the rat muscles exceeded the range of 30 mg, which can be kept in good physiological condition by superfusion with oxygenated physiological salt solution (PSS), and because their shape was inappropriate for our NMR methods, the rat DPH and TFL were split by blunt dissection along the axis of the fibers. All preparations had a maximal thickness of <1 mm. Only the middle portions of the muscle were laid in the sensitive volume of the coil such that attachment regions did not contribute to the spectral signal. All muscles were kept in PSS equilibrated with 100% O_2 and contained 116 mM NaCl, 4.6 mM KCl, 26.2 mM Mops (titrated to pH 7.4 with NaOH), 2.5 mM $CaCl_2$, 1.2 mM $MgSO_4$, and gentamycin (10 mg/l) at pH 7.4.

Muscles were frozen between brass blocks cooled to −196°C after the completion of spectral acquisition. When the muscles were put into the NMR probe, muscles from the

Abbreviations: DPH, diaphragm muscle; EDL, extensor digitorum longus muscle; PCr, phosphocreatine; TCr, total creatine (the sum of creatine plus phosphocreatine); SOL, soleus muscle; TFL, tensor fascia lata muscle.
‡To whom reprint requests should be addressed at: Department of Radiology, SB-05, University of Washington Medical Center, Seattle, WA 98195.

Table 1.   Volume fraction of fiber types

Muscle	Fiber type				Ref(s).
	2b	2a	2x	1	
Rat TFL	1.0	0	0	0	11
Rat EDL	0.85	0.13	0	0.02	11
Rat DPH	0.07	0.35	0.33	0.25	22
Rat SOL	0	0.1	0	0.9	11
Mouse EDL	0.63	0	0.36	0.01	13, 18
Mouse SOL	0	0	0.63	0.37	13, 23

Fractional volumes were obtained from data from the references cited. Note that the Gorza paper (13) shows that the mouse fibers previously classified as 2b are really 2x, whereas those previously classified as 2a are really 2b, so the data from Crow and Kushmerick (18) and Moerland *et al.* (23) were altered accordingly.

opposite limb were prepared similarly as a control. These control muscles, frozen about 30–45 min after dissection rather than after 1–2 hr in the NMR probe, showed no differences in HPLC content (data not shown). These preparations gave reproducible ^{31}P NMR spectra for up to 3 hr. HPLC data reported here were obtained from muscles frozen after completion of the NMR spectroscopy.

NMR Spectroscopy. Spectroscopy of the rat muscles was performed on a 8.5-T high-field spectrometer built by the Francis Bitter National Magnet Laboratory (Mass. Inst. Technol.); studies of the mouse muscles were made on a 7-T GN300 General Electric Omega spectrometer (University of Washington). The solenoidal coils used were tuned with a balanced tank circuit to the phosphorus frequency (145 MHz at 8.5 T; 121 MHz at 7 T) and attached to the probe constructed from aluminum and brass. An eight-turn solenoid of 30-gauge wire was used around a 1.5-mm i.d. capillary tube for the mouse muscle experiments; the coil was a six-turn solenoid of 22-gauge wire on a 2-mm i.d. capillary for the rat muscles. The unloaded Q of the resonant circuit (Larmor frequency divided by the full peak width at half maximum, $\approx$120) was reduced by $\approx$50% by loading with muscle and PSS for the larger diameter probe, but the loading was less ($\approx$20%) with the smaller one. The capillary was fixed horizontally in the apparatus, which provided reservoirs at both ends for the superfusate, as well as a mechanically stable foundation for the coil. PSS flow at 25 ± 2°C was usually 0.5 ml/min, which resulted in a flow velocity of superfusate over the surface of the muscle of $\approx$4 cm/sec. With a 140 mM Na$_2$HPO$_4$ standard in the smaller capillary (as used for the mouse muscle experiments), the signal-to-noise ratio for a single acquisition (π/2 pulse, sweep width of 5000 Hz, no exponential filtering) was 12:1.

Magnetic field homogeneity was optimized by shimming on the available proton signal from the sample (muscle and superfusate water). The linewidths for ^{1}H were usually in the range of 0.1–0.2 ppm for the rat muscles and usually <0.1 ppm for the mouse muscles. The π/2 pulse duration at a nominal power of 50 W was measured for each preparation and ranged between 4 and 10 μsec. Phosphorus spectra were obtained under fully relaxed and partial saturation conditions. Acquisition parameters were 2000 complex points, 5-kHz sweep width, 90° pulse, and 12-s recycle delay for fully relaxed spectra (15-s delay for the rat muscles) and a 45° pulse and 2-s recycle delay (90° pulse and 3-s recycle delay for the mouse muscles) for partly saturated spectra. For the mouse muscles, the saturation factor for the P$_i$ peak was 1.8; for PCr the factor was 1.4. For the rat muscles, the saturation factor for P$_i$ peak was 2.2; for PCr the factor was 1.05. Data were filtered by a 15-Hz exponential and zero-filled once prior to Fourier transformation. After acquisition of phosphorus spectra, muscles were rapidly removed from the probe, blotted, frozen, and stored at −80°C for later perchloric acid extraction and HPLC analysis as described (18, 20, 24). The

spectral peaks were integrated by summing the digitized data symmetrically about each peak; the baseline was flat. Each integral value was expressed as the fraction of the total phosphorus integral in the spectrum. Relative spectral areas were converted into chemical content based on the HPLC-measured ATP content as described in Table 3. Table 6 displays cellular concentrations derived from chemical content per g of wet weight by using cellular water fractions measured previously (20).

Statistical Analyses. Regression analyses were performed with the SYSTAT computer program (25).

RESULTS

Composition of Individual Muscles. A representative ^{31}P NMR spectrum of mouse EDL and SOL is displayed in Fig.
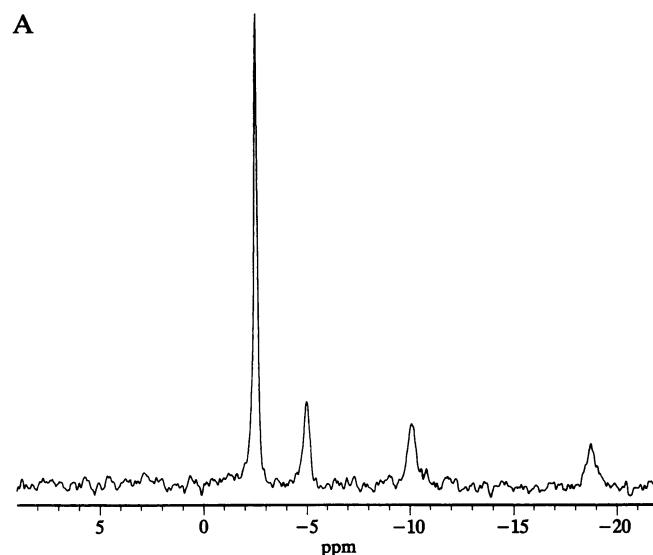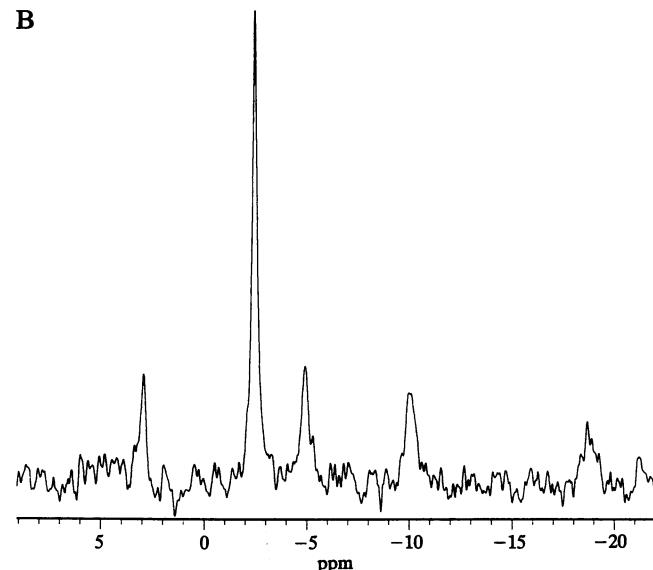

FIG. 1.   (*A*) Representative spectrum of a mouse EDL. Spectral intensity in arbitrary units is on the ordinate; chemical shift scale referenced to PCr = −2.54 ppm is on the abscissa. Acquisition parameters: 600 free induction decays, 2000 complex points, 5-kHz sweep, 90° pulse, 15-s recycle delay, and 15-Hz exponential filter. (*B*) Representative spectrum of a mouse SOL. Spectral intensity in arbitrary units is on the ordinate; chemical shift scale referenced to PCr = −2.54 ppm is on the abscissa. Acquisition parameters: 600 free induction decays, 2000 complex points, 5-kHz sweep, 90° pulse, 15-s recycle delay, and 15-Hz exponential filter.

1; spectral characteristics and quality were similar for the rat muscles. Note that a P_i peak was found only in one mouse EDL; a representative spectrum that shows the absence of a detectable P_i peak is given in Fig. 1. The fractional peak areas for all the muscles studied (peak area for each component of the spectrum divided by the sum of all peak areas adjusted for partial saturation) are given in Table 2. The spectral peak areas for each muscle were then divided by the average of the areas resulting from the γ phosphate of ATP (γ-ATP) and the β phosphate of ATP (β-ATP) (or in the case of the mouse muscle by the β-ATP peak) and multiplied by the ATP content measured by HPLC; resultant quantities for each metabolite are reported in Table 3 in units of μmol of metabolite content per g of wet weight.

Inspection of the data in Tables 2 and 3 with the fiber type composition of the muscles (Table 1) demonstrates that the content of P_i of muscles containing predominantly type 2b and 2a fibers was lower than in those containing primarily type 1 and 2x fibers: rat TFL $\approx$ EDL < DPH << SOL and mouse EDL << SOL. The content of PCr in muscles containing predominantly 2a and 2b fibers was higher than in those containing types 1 and 2x: rat TFL > EDL > DPH >> SOL and mouse EDL >> SOL. The ATP content was also clearly different in SOL compared to the others. The intracellular pH was 7.0–7.1 as calculated from the chemical shift of P_i with respect to PCr (data not shown), without any systematic differences in the muscles studied.

Quantitative Analysis of Fiber Type Composition and Metabolite Content. The metabolite composition characteristic of each of the fiber types given in Table 1 can be obtained by combining the data in Tables 1 and 3 into a matrix of simultaneous linear equations of the form:

$$[S]_i = \alpha_i(vf_{2b}) + \beta_i(vf_{2b}) + \gamma_i(vf_{2x}) + \delta_i(vf_1), \qquad [1]$$

where the subscript i refers to each of the four metabolites [total creatine (TCr), ATP, P_i, and PCr]; [S] is the measured whole muscle metabolite content; and the terms vf_{2b}, vf_{2a}, vf_{2x}, and vf_1 refer to volume fractions, respectively, of type 2b, 2a, 2x, and 1 fibers in each muscle. Coefficients α, β, γ, and δ represent the fiber-specific content of each ith metabolite, respectively, for type 2b, 2a, 2x, and 1 fibers. The solution of this matrix of equations was conveniently solved by treating Eq. 1 (and others that follow) as a problem of multiple regression analysis. The results of this analysis for TCr (PCr plus creatine) yielded the following coefficients (and their standard errors): α = 30.8 (2.0) μmol/g of wet weight of fiber for fiber type 2b; β = 28.2 (8.9) μmol/g of wet weight of fiber for type 2a; γ = 18.9 (4.1) μmol/g of wet weight of fiber for type 2x; and δ = 16.0 (3.4) μmol/g of wet weight of fiber for type 1. Analysis for ATP yielded α = 6.1 (0.1), β = 10.7 (0.6), γ = 3.5 (0.3), and δ = 3.2 (0.2) μmol/g of wet weight of fiber. The TCr and ATP contents of fiber type 1 were clearly smaller than those in type 2 fibers. The composition of type 2x fibers appeared more similar to the composition of type 1 fibers than to the metabolite contents

of types 2b and 2a; this hypothesis is tested below. Thus the null hypothesis (that all fiber types have the same resting composition) is excluded by the results of the first regression model.

We tested a second hypothesis, that the metabolite composition of type 2b, 2a, and 2x fibers are similar to each other but are different from type 1, by a second multiple regression model that grouped all the type 2 fibers into one class:

$$[S]_i = \theta_i(vf_{2b} + vf_{2a} + vf_{2x}) + \eta_i(vf_1), \qquad [2]$$

where the coefficient θ represents the ith metabolite content of fiber types 2b, 2a, and 2x postulated to be common to those three types and η represents the ith metabolite content of type 1 fibers. Results obtained are given in Table 4. Similarly we tested a third hypothesis (Table 4), that fiber types 2x and 1 have common metabolite contents, but that the composition is different from that of fiber types 2a and 2b. The regression model for this hypothesis is

$$[S]_i = \kappa_i(vf_{2b} + vf_{2a}) + \lambda_i(vf_{2x} + vf_1), \qquad [3]$$

where the coefficient κ represents the ith metabolite content of fiber types 2b and 2a and the coefficient λ represents the ith metabolite content of type 1 and 2x fibers.

Evidence favoring the third hypothesis (i.e., that type 1 and 2x fibers have the same composition and this composition is different from that of type 2a and 2b fibers) over the second hypothesis is the better statistical fit (judged from the magnitude of the F ratios given in Table 4) for the third regression model (Eq. 3) compared to the second (Eq. 2). There is a large difference between the postulated metabolite content of type 2x fibers according to hypotheses 2 and 3, and there are no type 2b or 2a fibers in mouse SOL (Table 1). Table 5 shows that regression model 3 is a much better predictor of the measured metabolite content of the mouse SOL than is model 2. Therefore hypothesis 2 is rejected. Finally we used regression models 2 and 3, which obviously were derived from the rat and mouse data in the present work, to predict the composition of cat biceps and SOL previously measured (20); the composition of the cat muscles was better predicted by regression model 3 than by model 2 (see Table 5).

DISCUSSION

The first conclusion from this work is that for all types of skeletal muscle the β-ATP peak area constitutes 13% of the total observable ^{31}P spectral area. To estimate normal muscle metabolite content by normalizing spectral areas of the observable peaks to that of ATP, one can use $\approx$7 μmol/g (for a predominantly fast-twitch muscle) or $\approx$4 μmol/g (for a slow-twitch muscle) as values for the ATP content per g of wet weight. Reports of muscle ATP content in a variety of muscle biopsies of human and experimental animals typically fall into the range quoted (26, 27). Obviously, in any particular muscle, and especially in situations of muscle pathology,

Table 2. Analysis of spectra of rat skeletal muscles

| Metabolite | Fractional peak areas from ^{31}P spectra | | | | | |
	Rat TFL	Rat EDL	Rat DPH	Rat SOL	Mouse EDL	Mouse SOL
P_i	0.03 ± 0.01	0.02 ± 0.0	0.05 ± 0.02	0.12 ± 0.02	0*	0.20 ± 0.02
PCr	0.53 ± 0.01	0.48 ± 0.01	0.44 ± 0.02	0.39 ± 0.01	0.53 ± 0.02	0.39 ± 0.03
γATP	0.13 ± 0.0	0.16 ± 0.01	0.16 ± 0.0	0.15 ± 0.01	0.13 ± 0.01	0.13 ± 0.01
αATP	0.19 ± 0.01	0.21 ± 0.01	0.23 ± 0.01	0.21 ± 0.01	0.18 ± 0.01	0.16 ± 0.01
βATP	0.11 ± 0.0	0.13 ± 0.0	0.11 ± 0.01	0.13 ± 0.01	0.14 ± 0.01	0.12 ± 0.01
P_i/PCr	0.06	0.04	0.11	0.31	0.09	0.51

Values given are the mean (±1 SE; n = 5) relative peak areas of each species as a fraction of the summed areas of all the detected peaks. SE values stated as 0.0 means that the value was <0.005.
*The P_i area was detectable in only one mouse EDL, which had a value of 0.048.

Table 3. Analysis of metabolite content of skeletal muscles

Metabolite	Chemical content, μmol/g					
	Rat TFL	Rat EDL	Rat DPH	Rat SOL	Mouse EDL	Mouse SOL
TCr	29.8 ± 3.8	28.9 ± 1.0	22.5 ± 1.0	17.9 ± 1.1	29.5 ± 1.1	15.9 ± 0.6
ATP	5.9 ± 0.5	6.7 ± 0.2	6.1 ± 0.5	4.0 ± 0.2	5.3 ± 0.4	3.3 ± 0.1
P_i	1.8 ± 0.7	1.1 ± 0.2	2.3 ± 0.7	3.6 ± 0.8	0*	6.0 ± 1.3
PCr	26.8 ± 0.2	22.7 ± 1.3	20.1 ± 1.1	11.2 ± 0.8	21.1 ± 2.9	11.4 ± 1.6

ATP and TCr contents are HPLC analyses of perchloric acid extracts of rapidly frozen samples normalized to frozen weight. This measure of ATP was used to calibrate the spectral analyses displayed in Table 2 to calculate the contents of P_i and PCr in terms of weight from the spectra. The values given are the means ± 1 SE ($n = 5$).
*No P_i was detected; see Table 2.

confirmation by direct analyses from biopsies or by a method of absolute NMR calibration is required.

It is possible that the results from the muscles *in vitro* systematically differ from their composition in the intact animal because of incubation conditions or damage during preparation. The following comparison shows no evidence for such differences. Rat lower limb musculature was sampled by a surface coil (28) in a way that sampled types 2a and 2b, mixed fast muscle (29). The PCr/ATP ratio from table 1 of that paper (the ATP value was calculated in the same way as in our experiments) was 3.6, and the P_i/PCr ratio was 0.10. Both values are similar to the present data in Table 2 for muscles composed predominantly of those muscle types. The P_i/PCr ratios in the present data are not higher, and the PCr/ATP ratios are not lower, as would have been expected if some systematic difference in the *in vitro* muscles led to an artifactual result.

The main conclusion relates to important differences between the composition of the specific fiber types. Our analyses indicate that categories based upon the intracellular content of bioenergetically important metabolites, PCr, ATP, P_i, and TCr, do not necessarily correspond to other schemes of classifying fiber types, which were summarized in the Introduction. Type 2a and 2b fibers appear to have slight differences in chemical content and therefore in their spectral characteristics at rest. The content of type 1 fibers was clearly different from that of types 2b and 2a. The composition of type 2x fibers was more similar to type 1 fibers than to the other type 2 fibers. The conclusion of grouping type 2x and type 1 fibers into the same compositional class was unexpected because 2x fibers are mechanically fast (8). The P_i content of whole muscles increased while the PCr content decreased with increasing content of type 1 and 2x fibers. These results were seen in the rat DPH and were especially prominent in the mouse SOL. We found about a 10-fold range in the P_i/PCr ratios in normal resting muscles, from 0.05 (or lower) in fast-twitch fibers (types 2a and 2b) to 0.5 in muscles containing predominantly type 1 and 2x fibers.

Table 4. Regression analysis predicting compositions of specific fiber types

Parameter	Chemical content, μmol/g of wet weight			
	TCr	ATP	P_i	PCr
Regression model 2				
θ	27.8 ± 2.1	5.9 ± 0.6	1.5 ± 1.0	22.8 ± 2.0
η	13.3 ± 4.1	3.3 ± 1.1	5.2 ± 1.9	7.6 ± 3.9
F ratio	111	72	6.4	80
Regression model 3				
κ	30.7 ± 1.4	6.5 ± 0.5	0.6 ± 0.9	25.6 ± 1.4
λ	16.9 ± 1.5	3.8 ± 0.5	4.5 ± 1.0	11.6 ± 1.5
F ratio	373	163	11	245

Values given are the means ± SE. For regression model 2, the compositions of type 2b, 2a, and 2x fibers are postulated to be similar to each other but different from type 1. For regression model 3, fiber types 2x and 1 are postulated to have common metabolite contents but different from those of fiber types 2a and 2b.

The third conclusion is that the results obtained from murine muscles extend to other mammalian skeletal muscles. In Table 5 our analysis and conclusions concerning fiber-type composition observed in the rat and mouse predicted accurately the composition of cat biceps and SOL previously measured. Because the results obtained herein may be representative of mammalian fibers in general, we recalculated the data in terms of intracellular metabolite concentration to yield our best estimate of the TCr, ATP, PCr, P_i, and ADP cellular concentration in the two classes of mammalian fibers and the Gibbs free energy available from ATP. This summary appears in Table 6.

It remains an open question why the content of phosphate-containing metabolites differs in these fiber types. It is possible that the content of metabolites observed is related to the fiber's capacity for oxidative metabolism. However, this cannot be the complete explanation because fiber types 2a and 2b, which differ in their oxidative capacity, were indistinguishable. These cells are subject to the same extrinsic hormonal regulation and extracellular fluid composition in the animal, so differences in cellular content appear to be a genuine phenotypic distinction between muscle cells. We have speculated that differing steady-state compositions of bioenergetically important phosphate compounds (which can be altered by exercise and, in experimental animals, by chronic stimulation and by uptake of creatine analogs) may be an important factor influencing the muscle's phenotype (23), although a causal relationship has not been established. However, our interpretation of fiber type-specific composi-

Table 5. Comparison of observed and predicted chemical compositions of skeletal muscles

Metabolite	Chemical content, μmol/g of wet weight		
	Predicted		Observed
	Hypothesis 2	Hypothesis 3	
Mouse SOL			
TCr	22.4	16.9	15.9 (0.5)
PCr	17.2	11.6	11.4 (1.6)
ATP	4.9	3.8	3.3 (0.1)
P_i	2.9	4.5	6.0 (1.3)
Cat biceps			
TCr	27.8	30.7	27.7
PCr	22.8	25.6	27.6
ATP	5.9	6.5	7.0
P_i	1.5	0.6	2.4
Cat SOL			
TCr	13.3	16.9	17.8
PCr	7.6	11.6	12.1
ATP	3.3	3.8	3.7
P_i	5.2	4.5	7.4

Observed data are from Table 3 for rat and mouse muscles and from ref. 20 for cat muscles; it is not known whether type 2x fibers are found in cat biceps and SOL. Hypothesis 2 is given by Eq. 2: type 1 different from type 2b = 2a = 2x. Hypothesis 3 is given by Eq. 3: type 1 = type 2x and type 2b = 2a.

Physiology: Kushmerick *et al.*

Proc. Natl. Acad. Sci. USA **89** (1992)   7525

Table 6. Composition of murine fiber types

Metabolite	Types 2a and 2b	Types 1 and 2x
TCr, mM	39	23
PCr, mM	32	16
P_i, mM	0.8	6
ATP, mM	8	5
ADP, μM	8	11
μATP_{obs}, $-kJ/mol$	68	61

These estimates were obtained as explained in the text from multiple regression analyses. ADP and the Gibbs free energy were calculated (20) from mean values of PCr, ATP, TCr, and P_i with a common intracellular pH = 7.0 with the quantities given in Table 3.

tion is clearly different from that of Hintz *et al.* (21). Thus it is not necessary to have different degrees of muscle activity to observe differences in PCr, P_i, and ADP contents.

P_i inhibits isometric force in permeabilized single-fiber preparations (30–32), with a half-maximal inhibition in the several millimolar range. Type 1 and 2x fibers have a P_i content that would be inhibitory of actomyosin interactions producing force from the beginning of contractile activity. It could be a useful strategy to arrange a cellular milieu such that the concentration of this inhibitory metabolite changes relatively little with respect to its inhibitory constant, as would be the case for type 1 and 2x fibers at the concentration of P_i we measured. Metabolic fatigue attributable to changes in P_i concentration would then be quite small in types 1 and 2x compared to that in the other fiber types. A possible survival benefit of this type of strategy could be that the primary consideration is the maintenance of mechanical output even at a cost of partial inhibition. The mechanical power output of these fibers, whenever activated, would be diminished relative to their maximal potential, but their actual function would be maintained during prolonged activity by two mechanisms: (*i*) energy balance is more easily achieved by a higher ATP synthesis rate relative to the ATP demand, and (*ii*) any further change in P_i concentration would result in little reduction in mechanical power output.

The extent of changes in high-energy phosphate compounds in type 2a and 2b fibers during contractile activity (and the rates of their recovery to resting levels) will be substantially different from that of type 1 and 2x fibers. Similar reasoning argues that, although the resting contents of type 2x and 1 fibers are similar at rest, their contents will also diverge during muscular activity because of the greater ATPase rate [inferred from their high velocity of shortening (8) compared to that of slow-twitch type 1 fibers]. Thus any heterogeneity of metabolite content existing in resting muscle is likely to change with a complex time course during and after muscle contraction because of the differences in the magnitude of cellular ATPase activity and capacity for oxidative ATP synthesis. Without quantitative knowledge of the energetic characteristics of and dynamic changes in the constituent muscle fibers with respect to the components of energy balance (namely, ATPase rate and ATP synthesis rate), the interpretation of chemical changes by ^{31}P NMR spectroscopy or other macroscopic methods will remain ambiguous.

1. Saltin, B. & Gollnick, P. D. (1983) in *Handbook of Physiology: Skeletal Muscle*, ed. Peachey, L. D. (Am. Physiol. Soc., Bethesda, MD), Sec. 10, pp. 555–631.
2. Henneman, E., Somjen, G. & Carpenter, D. O. (1965) *J. Neurophysiol.* **28**, 560–580.
3. Burke, R. E. & Edgerton, V. R. (1975) *Exercise Sport Sci. Rev.* **3**, 31–81.
4. Lewis, D., Parry, D. & Rowlerson, A. (1982) *J. Physiol.* **325**, 393–401.
5. Peter, J. B., Barnard, R. J., Edgerton, V. R., Gillespie, C. A. & Stempel, K. E. (1972) *Biochem.* **11**, 2627–2633.
6. Ariano, M. A., Armstrong, R. H. & Edgerton, V. R. (1973) *J. Histochem. Cytochem.* **21**, 51–55.
7. Burke, R. E., Levine, D. N., Tsairis, P. & Zajac, F. E., III (1973) *J. Physiol.* **234**, 723–748.
8. Bottinelli, R., Schiaffino, S. & Reggiani, C. (1991) *J. Physiol.* **437**, 655–672.
9. Sweeney, H. L., Kushmerick, M. J., Mabuchi, K., Sreter, F. A. & Gergely, J. (1988) *J. Biol. Chem.* **263**, 9034–9039.
10. Metzger, J. M. & Moss, R. L. (1987) *Biophys. J.* **52**, 127–131.
11. Tsika, R. W., Herrick, R. E. & Baldwin, K. M. (1987) *J. Appl. Physiol.* **63**, 2101–2110.
12. Ausoni, S., Gorza, L., Schiaffino, S., Gundersen, K. & Lomo, T. (1990) *J. Neurosci.* **10**, 153–160.
13. Gorza, L. (1990) *J. Histochem. Cytochem.* **38**, 257–265.
14. Maier, A., Gorza, L., Schiaffino, S. & Pette, D. (1988) *Cell Tissue Res.* **254**, 59–68.
15. LaFramboise, W., Daood, M., Guthrie, R., Moretti, P., Schiaffino, S. & Ontell, M. (1990) *Biochim. Biophys. Acta* **1035**, 109–112.
16. LaFramboise, W., Daood, M., Guthrie, R., Schiaffino, S., Moretti, P., Brozanski, B., Ontell, M., Butler-Browne, G., Whalen, R. & Ontell, M. (1991) *Dev. Biol.* **114**, 1–15.
17. Pette, D. & Staron, R. S. (1990) *Rev. Physiol. Biochem. Pharmacol.* **116**, 1–76.
18. Crow, M. T. & Kushmerick, M. J. (1982) *J. Gen. Physiol.* **79**, 147–166.
19. Ranvier, L. (1874) *Arch. Physiol. Norm. Pathol.* **1**, 5–15.
20. Meyer, R. A., Brown, T. R. & Kushmerick, M. J. (1985) *Am. J. Physiol.* **248**, C279–C287.
21. Hintz, C. S., Chi, M. M.-Y., Fell, R. D., Ivy, J. L., Kaiser, K. K., Lowry, C. V. & Lowry, O. H. (1982) *Am. J. Physiol.* **242**, C218–C228.
22. LaFramboise, W. A., Watchko, J. F., Brozanski, B. S., Daood, M. J. & Guthrie, R. D. (1992) *Am. J. Respir. Cell Mol. Biol.* **6**, 335–339.
23. Moerland, T. S., Wolf, N. G. & Kushmerick, M. J. (1989) *Am. J. Physiol.* **257**, C810–C816.
24. Wiseman, R. W., Moerland, T. S., Chase, P. B., Stuppard, R. & Kushmerick, M. J. (1992) *Anal. Biochem.*, in press.
25. Wilkinson, L. (1989) *SYSTAT: The System for Statistics* (SYSTAT, Evanston, IL).
26. Ren, J.-M. & Hultman, E. (1989) *J. Appl. Physiol.* **67**, 2243–2248.
27. Gollnick, P. D., Armstrong, R. B., Sembrowich, W. L., Shepherd, R. E. & Saltin, B. (1973) *J. Appl. Physiol.* **34**, 615–618.
28. Kushmerick, M. & Meyer, R. (1985) *Am. J. Physiol.* **248**, C279–C287.
29. Armstrong, R. B. & Phelps, R. O. (1984) *Am. J. Anat.* **171**, 259–272.
30. Cooke, R. & Pate, E. (1985) *Biophys. J.* **48**, 789–798.
31. Godt, R. E. & Nosek, T. M. (1989) *J. Physiol.* **412**, 155–180.
32. Millar, N. C. & Homsher, E. (1990) *J. Biol. Chem.* **265**, 20234–20240.